



Design Optimization of a Permanent Magnet Generator for Direct Drive Wind Turbine

A. Jabbari*, M. Basaki, M. R. Sheykholeslami

Manufacturing and Production Department, Faculty of Engineering, Arak University, Arak, Iran

PAPER INFO

Paper history:

Received 05 August 2023

Accepted in revised form 01 November 2023

Keywords:

Axial flux generator
Design optimization
Experimental study
Gearless wind turbine
Numerical study

ABSTRACT

In this paper, an axial flux permanent magnet generator for a 30 kW direct drive wind turbine is designed and the design parameters were optimized with the aim of achieving high efficiency. In order to reduce the cogging torque and electromagnetic torque ripple components, the air core topology has been used, and with the aim of increasing the power capacity of the generator, a modular structure has been used. The advantage of the modular design is that each module can be considered as a generator unit and depending on the wind speed conditions, the number of units corresponding to the wind speed can be placed in the circuit and the generator will always work with maximum efficiency. First, by using the governing equations, the dimensions and performance characteristics of the generator are determined, and then a generator prototype is fabricated based on the electromagnetic design. In order to evaluate the output performance of the generator, machine simulation was performed in Maxwell finite element analysis software and the characteristic curves of voltage, current and ohmic losses were extracted. In order to evaluate the accuracy of the results, the outcomes of the analytical method have been compared with the experimental tests results.

Doi: 10.5829/ijee.2024.15.03.03

INTRODUCTION

Brushless permanent magnet electric machines are primary generators for distributed generation systems. These self-excitation generators are compact and have high reliability and efficiency. Any electric power generation technology that is integrated into a distribution system is called distributed generation. Dispersed production technologies are divided into two categories: renewable and non-renewable. Renewable technologies include solar, photovoltaic, thermal, wind, geothermal and ocean as energy sources.

Axial Flux Permanent Magnet (AFPM) brushless generators can be used both as high-speed generators in gas turbines and as low-speed generators in hydro and wind turbines. Their advantages are high power density, modular structure, high efficiency and easy integration with other mechanical components such as turbine rotors.

A low speed AFPM generator is usually driven by a wind turbine. With wind energy rapidly becoming one of the most desirable alternative energy sources in the worldwide, AFPM generators offer a very low-cost solution compared to solar cells.

Brushless permanent magnet machines without stator and rotor cores were first used in the late 1990s in industrial electromechanical servo mechanisms and drives [1], solar powered electric vehicles [2], as well as micro-motors for computer peripherals and vibration motors for mobile phones [3], were made commercially.

Axial permanent magnet generators have different types of topologies, according to the user requirements in wind turbines without gearboxes, multi-disc topologies with non-ferrous stator cores and a combination of air and iron cores are used for the rotor.

With high energy magnets, it is possible to make the stators and rotors of AFPM brushless machines without ferromagnetic cores [1-5]. A completely coreless design reduces mass and increases machine efficiency compared to a conventional design. Besides, a coreless AFPM brushless machine produces no normal force of attraction between the stator and the rotor and produces no torque pulses in the zero current condition.

There is a limitation in increasing the electromagnetic torque that is obtained by enlarging the diameter of the machine. In the design of an axial permanent magnet motor disk, due to some limiting factors, it is not possible

*Corresponding Author Email: a-jabbari@araku.ac.ir (A. Jabbari)

to increase the diameter of the motor to achieve a higher torque. The factors limiting the design of a disc are: axial force applied to the bearings, the integrity of the mechanical connection between the disc and the spindle, disc stiffness.

In previous studies, an analytical method based on the subdomain technique was proposed to determine the performance characteristics of permanent magnet machines [6-23]. In this research, design and fabrication of a 30 kW axial flux permanent magnet brushless generator has been considered for a gearless wind turbine. Initial design has been performed based on governing equations, assumptions and restrictions. The results of analytical method has been compared and validated by FEM analysis. A prototype axial flux permanent magnet generator has been fabricated based on optimum results and its performance has been tested using an experimental setup. It is shown that FEM results are in good agreement with the experimental results.

MATERIAL AND METHODS

Topology and construction

A logical solution for high torques is two or more disk generators. There are several combinations of multi-disc motors [24-28]. A schematic of the proposed AFPM brushless generator for use in gearless wind turbine with a blade length of 8 meters is shown in Figure 1. In this design, the rotor consists of 9 permanent magnet plates, 7 of which have an air core (made of Plexiglas) and 2 of which have iron cores, which are connected to each other by screws and installed on the generator shaft. Also, 8 stator plates are installed on the rings of the generator shell on the spacers between the rotors. These plates are also non-ferrous and made of Plexiglas plates. The three-phase stator windings are assembled concentrically like flower petals. The coils are arranged in overlapping layers around the axis of the machine. Then the entire coil is placed in a plastic or resin with high mechanical strength. Since no grooved ferromagnetic core is used in the topology shown in Figure 1 in the stator structure, the cogging torque phenomenon and core losses do not exist. The only loss components are eddy current and losses in the stator winding conductors.

This modular design helps to easily increase the shaft power output to the desired level by adding more units. In this design, the turbine hub is directly connected to the generator shaft without the need for a gearbox.

Electromagnetic design

A three-phase Y-connected low-speed brushless AFPM generator, with a rated power of 30 kW and a rated speed of 150 rpm, is designed. The 7 air core rotor plates (without ferromagnetic core) and 2 rotor plates have a steel backing plate. The 8 stator plates include round coils embedded in Plexiglas plates. Medium quality sintered

NdFeB permanent magnets with $B_r=1.2$ and $H_c=950$ kA/m have been used. Design data and calculated parameters are given in Table 1.

In this section, the governing equations for calculating the magnetic flux density of the air gap, the electromagnetic moment, and the electric driving force of the generator are stated.

Airgap flux density distribution

Two-dimensional FEM modeling of the magnetic field in the air gap of the coreless AFPM brushless machine has

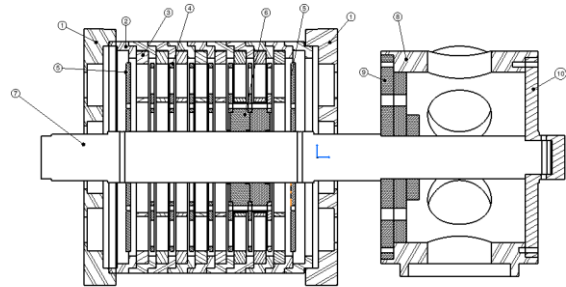


Figure 1. A schematic representation of the proposed modular axial flux generator for 30kW gearless wind turbine

Table 1. The axial flux generator characteristics

Parameter	Unit	Value
Rated speed	rpm	500
Rated power	W	30000
Phase No.		3
Pole No.		16
No. of coils		12
Rated frequency	Hz	66.67
Magnet type		NdFeB
Magnet Diameter	mm	65
Magnet thickness	mm	8
Magnet pitch at mean diameter	mm	70
Pole pitch	deg	22.5
Rotor thickness	mm	10
Overall diameter	mm	495
Axial length	mm	67
Stator thickness	mm	20
Coil pitch	deg	30
Coil outer diameter	mm	75
Coil inner diameter	mm	30
Coil height	mm	14
Wire diameter	mm	1
Number of coils wire		276

been carried out. NdFeB magnets with residual flux density $B_r=1.2\text{T}$ and hysteresis $H_c=950\text{kA/m}$ are considered. The thickness of each permanent magnet is assumed to be 10 mm, the thickness of the coreless stator winding is 19 mm, and the thickness of the air gap of one side is 2 mm.

The peak value of the normal component of the high magnetic flux density (above 0.6 T) has been stimulated. This value is enough to obtain a high electromagnetic torque. The peak flux density value for the optimal magnetic circuit of an AFPM machine can be even higher.

Electromagnetic torque

The electromagnetic torque of an AFPM brushless machine can be calculated based on Equations 1-5. Also, EMF can be calculated according to Equations 6-9. The average torque is equal to:

$$T_d = 2 \frac{p}{\pi} m_1 N_1 k_{\omega 1} \Phi_f I_a \quad [1]$$

From the product of Equation 1 at the value of $\pi \sqrt{2}/2 \approx 2.22$, the rms torque for current and sinusoidal magnetic flux density is obtained:

$$T_d = \frac{m_1}{\sqrt{2}} p N_1 k_{\omega 1} \Phi_f I_a = k_T I_a \quad [2]$$

where is the torque constant is

$$k_T = \frac{m_1}{\sqrt{2}} p N_1 k_{\omega 1} \Phi_f \quad [3]$$

The electromagnetic torque of the generator is

$$T_d = \frac{p_{elm}}{2\pi n} = \frac{E_{fL-L} I_a^{(sq)}}{2\pi n} = \frac{4}{\pi} p N_1 k_{\omega 1} \Phi_f^{(sq)} I_a^{(sq)} = k_{Tdc} I_a^{(sq)} \quad [4]$$

where the torque constant of a square wave machine is

$$k_{Tdc} = \frac{k_{Edc}}{2\pi} = \frac{4}{\pi} p N_1 k_{\omega 1} \Phi_f^{(sq)} \quad [5]$$

Also, EMF can be calculated according to Equations 6-9.

$$E_f = \pi \sqrt{2} f N_1 k_{\omega 1} \Phi_f = \pi \sqrt{2} p N_1 k_{\omega 1} \Phi_f n_s = k_E n_s \quad [6]$$

where is the constant EMF (armature constant) is

$$k_E = \pi \sqrt{2} p N_1 k_{\omega 1} \Phi_f \quad [7]$$

For the Y-connection of the armature windings, as shown in Figure 2, two phases carry current at the same time. The line-to-line emf of a Y-connected square wave motor is

$$E_{fL-L} = 2e_f = 8pN_1k_{\omega 1}\alpha_i^{(sq)}B_{mg}\left(\frac{\pi}{2p}\right)(R_{out}^2 - R_{in}^2)n = 8pN_1k_{\omega 1}\Phi_f^{(sq)}n = k_{Edc}n \quad [8]$$

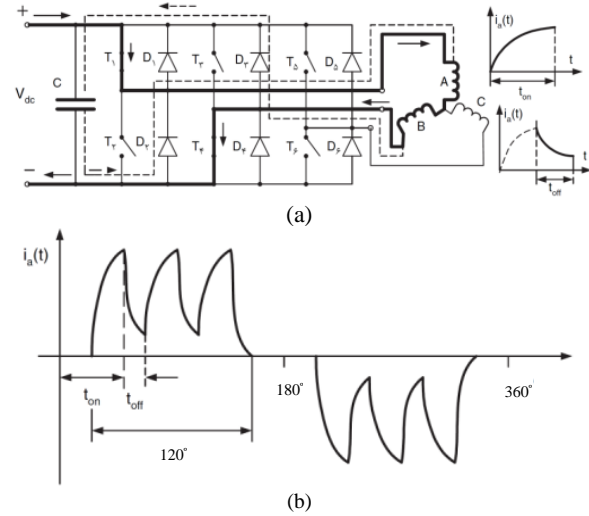


Figure 2. Inverter currents at stator windings of a brushless machine. (a) Currents in A and B phases, (b) rectangular waveform

Generator fabrication

Based on the design shown in Figure 1 as well as the geometric dimensions obtained from the analysis of the generator performance according to the requirements of the desired wind turbine, this section describes the manufacturing process of the various components of the generator.

In Figure 3, the software model of the rotor plate is shown. 16 NdFeB permanent magnets with grade N35 are installed in the rotor plate. In 7-Plexiglas plates, permanent magnets are installed inside the plate, and in two ferromagnetic plates, permanent magnets are installed on the plate at the beginning and end of the rotor according to Figure 4. This figure shows the ferromagnetic plate of the rotor backing.

Spacers are used to ensure the uniform spacing of the rotor plates and to bear the weight of these plates. Figure 5 shows the three-dimensional model of the rangefinder. To make the mass of the rotor light and reduce its inertia, cast aluminum has been used to make the spacers.

Each stator block is made of two Plexiglas plates, 12 coils of wire and an aluminum ring. These components are shown in Figure 6.

The stepped aluminum rings shown in Figure 7 are used to precisely position the stator plates. The stepped feature allow the assembly of other rings and thus increase the number of stator blocks.

Each stator block is placed between two rotor discs and has 12 round armature coils. The stator windings has 12 non-overlapping concentric coils, that is, 4 coils

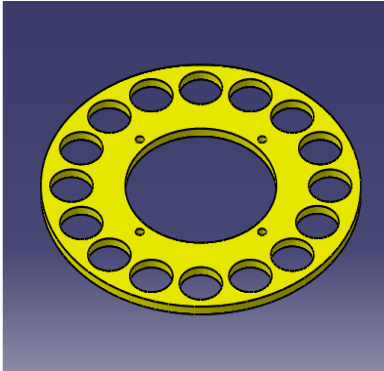


Figure 3. The stator plate model



Figure 4. The back-iron of the rotor

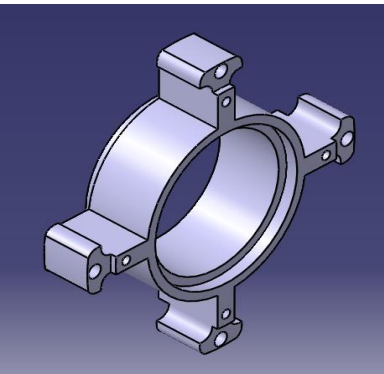


Figure 5. A CAD model of spacers

per phase. The thickness of each coil is 19 mm and the diameter of the wire is 1 mm. The current of each coil is rectified separately to DC to reduce the ripple effect of the commutation torque and to perform a better control on the voltage.

The advantages of this type of generator include round coils have the shortest circumference and the least resistance; easy manufacturing and low production costs; easy assembly, because there are no magnetic forces between the rotor and the stator; Absence of cog torque and as a result low mechanical resistance in starting the turbine.

Figure 8 shows the model of the generator cover and the built cover. The cover material is selected from aluminum and after the casting process, machining operations have been performed on it. As can be seen in this figure, 4 holes have been installed on the cover of the generator to install external fans for better cooling of the generator.

During the assembly of different components of the generator, it is important to pay attention to some principles. When assembling the rotor plates, it is necessary to pay attention to the magnetic direction of the plates. This is also true for the assembly of the stator plates. So that according to the direction of the coils and the starting point of the phases, all the plates are installed similarly on the stator rings. From each stator block, 6 wires come out, which correspond to the



Figure 7. The stator rings after machining process



Figure 6. The fabricated stator plates

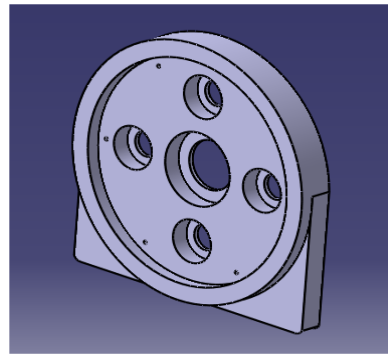


Figure 8. The generator endcap model

three phases of each block. If the ends of the wires are available, it is possible to connect the generator coils in a star, triangle or series and parallel combination.

RESULTS AND DISCUSSION

Analytical modeling

In Figure 9, the analytical modeling done in Maxwell software is shown. As can be seen, the number of poles is 16 and the number of rotor module is 8. The parameters of the generator are listed in Table 1. In this analysis, the generator performance characteristics such as magnetic flux density distribution, output phase voltage and phase current are determined in different speed and load conditions. Figure 10 shows the output voltage diagram and Figure 11 shows the current diagram in different phases of the generator at a speed of 390 rpm. Ohmic losses of the generator is also shown in Figure 12. A comparison of analytical and numerical results is listed in Table 2.

Experimental tests

Figure 13 shows the generator during testing on the lathe. To check the performance of the generator, due to its low rated speed, a lathe machine is used. Figures 14 and 15 show the output voltage and speed-voltage comparison at 390 rpm for analytical and experimental test results. The fabricated gearless wind turbine at Arak University is shown in Figure 16.

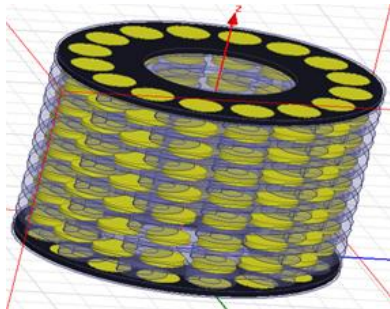


Figure 9. Simulation of the generator in Maxwell software

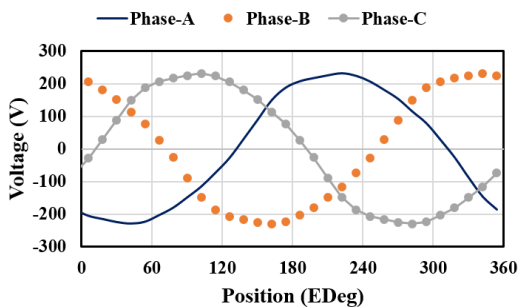


Figure 10. Output voltage waveform at 390 rpm

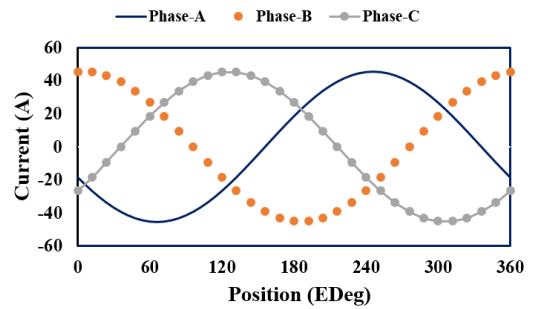


Figure 11. Output current waveform at 390 rpm

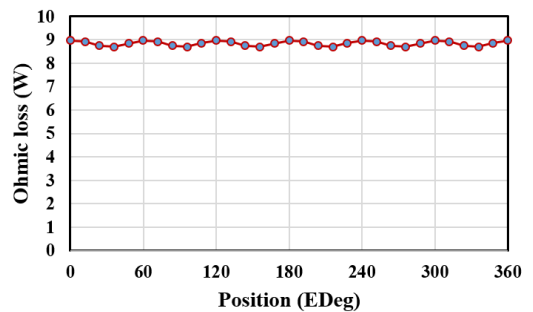


Figure 12. The generator ohmic losses

Table 2. A comparison of analytical and numerical results

Parameter	Unit	Analytical	Numerical	Error (%)
Current (Phase-A)	Amper	45.42	44.48	2.11
Current (Phase-B)	Amper	45.42	44.19	2.78
Current (Phase-C)	Amper	45.42	44.59	1.86
Voltage (Phase-A)	Volt	220	226.20	2.86
Voltage (Phase-B)	Volt	220	226.73	3.05
Voltage (Phase-C)	Volt	220	226.74	3.06
Ohmic loss	Watt	8623	9075	5.24
Efficiency	%	81.25	79.65	2

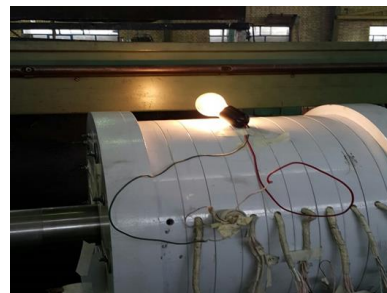


Figure 13. The fabricated generator test rigs

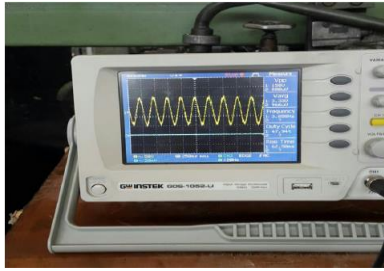


Figure 14. The generator output voltage at 390 rpm

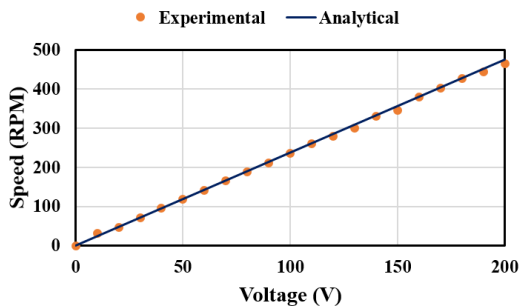


Figure 15. Speed-Voltage diagram. A comparison between experimental and analytical results



Figure 16. The fabricated wind turbine at arak university

CONCLUSION

Design, Optimization and fabrication of a prototype axial flux permanent magnet brushless generator for a 30 kW direct drive gearless wind turbine was described in this research paper. Initial geometrical design was carried out based on wind turbine requirements by using analytical equations and verified using FEA method and then

validated by experimental tests on the fabricated generator using a dynamometer. In order to evaluate the output performance of the generator, machine simulation was performed in Maxwell finite element analysis software and the characteristic curves of voltage, current and ohmic losses were extracted. In order to evaluate the accuracy of the results, the results of the analytical method have been compared with the experimental tests results. It is shown that maximum error percentage between analytical, numerical and experimental results is about 3 percent.

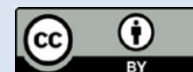
REFERENCES

- Soderlund L, Koski A, Vihriala H, Eriksson JT., Perala R. Design of an axial flux permanent magnet wind power generator. In 1997 Eighth International Conference on Electrical Machines and Drives. 1997 Sept; 444: 224-8. Doi: 10.1049/cp:19971072
- Lovatt HC, Ramsden VS, Mecrow BC. Design of an in-wheel motor for a solar-powered electric vehicle. IEE Proceedings-Electric Power Applications. 1998 Sep 1; 145(5):402-8. Doi: 10.1049/cp:19971074
- Xue X, Zhang Z, Wu B, He S, Wang Q, Zhang W, Bi R, Cui J, Zheng Y, Xue C. Coil-levitated hybrid generator for mechanical energy harvesting and wireless temperature and vibration monitoring. Science China Technological Sciences. 2021 Jun; 64(6): 1325-34. Doi: 10.1007/s11431-020-1755-4
- Gieras JF, Gieras IA. Performance analysis of a coreless permanent magnet brushless motor. In Conference Record of the 2002 IEEE Industry Applications Conference. 37th IAS Annual Meeting (Cat. No. 02CH37344) 2002 Oct 13; 4: 2477-82. Doi: 10.1109/IAS.2002.1042794
- Jamali Arand S, Ardebili M. Multi-objective design and prototyping of a low cogging torque axial-flux PM generator with segmented stator for small-scale direct-drive wind turbines. IET Electric Power Applications. 2016 Nov; 10(9): 889-99. Doi: 10.1049/iet-epa.2016.0007
- Tavakoli G, Jabbari A, Sheykhosslami MR. A semi-analytical, numerical and experimental study on performance characteristics of a novel hybrid-rotor CVT magnetic gearbox. Proceedings of the Institution of Mechanical Engineers, Part D: Journal of Automobile Engineering. 2023 Jul; 237(8): 1994-2005. Doi: 10.1177/09544070221103162
- Jabbari A. The Effect of dummy slots on machine performance in brushless permanent magnet machines: An analytical, numerical, and experimental study. Iranian Journal of Electrical & Electronic Engineering. 2022 Jun 1; 18(2). Doi: 10.22068/IJEEE.18.2.2284
- Jabbari A. Semi-analytical modeling of electromagnetic performances in magnet segmented Spoke-type permanent magnet Machine Considering Infinite and Finite Soft-Magnetic Material permeability. Iranian Journal of Electrical & Electronic Engineering. 2021 Mar 1; 17(1). Doi: 10.22068/IJEEE.17.1.1711
- Jabbari A, Dubas F. The Effect of magnet width and iron core relative permeability on iron pole radii ratio in Spoke-type permanent-magnet machine: An analytical, numerical and experimental study. Iranian Journal of Electrical and Electronic Engineering. 2021 Jun 10; 17(2): 1802. Doi: 10.22068/IJEEE.17.2.1802
- Jabbari A, Dubas F. An improved model for performances calculation in spoke-type permanent-magnet machines considering

- magnetization orientation and finite soft-magnetic material permeability. *COMPEL-The international journal for computation and mathematics in electrical and electronic engineering*. 2020 Dec 15; 39(6): 1299-314. Doi: 10.1108/COMPEL-08-2019-0326
11. Jabbari A, Taheri H, Ghadimi AA. An analytical, numerical and experimental study on performance characteristics in a novel Vernier permanent magnet machine. *Electrical Engineering*. 2020 Dec; 102: 2369-79. Doi: 10.1007/s00202-020-01035-1
 12. Jabbari A, Dubas F. A New Subdomain Method for Performances Computation in Interior Permanent-Magnet (IPM) Machines. *Iranian Journal of Electrical & Electronic Engineering*. 2020 Mar 1; 16(1). Doi: 10.22068/IJEEE.16.1.26
 13. Jabbari A, Dubas F. Analytical Modelling of Magnetic Field Distribution in Spoke Type Permanent Magnet Machines. *Journal of Iranian Association of Electrical and Electronics Engineers*. 2020;17(3):141-51. Doi: 20.1001.1.26765810.1399.17.3.2.8
 14. Jabbari A. Analytical modeling of magnetic field distribution in multiphase H-type stator core permanent magnet flux switching machines. *Iranian Journal of Science and Technology, Transactions of Electrical Engineering*. 2019 Jul 1; 43(Suppl 1): 389-401. Doi: 10.1007/s40998-018-0113-1
 15. Jabbari A. An analytical study on iron pole shape optimization in high-speed interior permanent magnet machines. *Iranian Journal of Science and Technology, Transactions of Electrical Engineering*. 2020 Mar; 44(1): 169-74. Doi: 10.1007/s40998-019-00217-3
 16. Jabbari A. An analytical expression for magnet shape optimization in surface-mounted permanent magnet machines. *Mathematical and Computational Applications*. 2018 Oct 5; 23(4): 57. Doi: 10.3390/mca23040057
 17. Jabbari A. Analytical modeling of magnetic field distribution in inner rotor brushless magnet segmented surface inset permanent magnet machines. *Iranian Journal of Electrical and Electronic Engineering*. 2018 Sep 10; 14(3): 259-69. Doi: 10.22068/IJEEE.14.3.259
 18. Jabbari A. Exact analytical modeling of magnetic vector potential in surface inset permanent magnet DC machines considering magnet segmentation. *Journal of Electrical Engineering*. 2018 Jan 1; 69(1): 39-45. Doi: 10.1515/jee-2018-0005
 19. Jabbari A. 2D analytical modeling of magnetic vector potential in surface mounted and surface inset permanent magnet machines. *Iranian Journal of Electrical and Electronic Engineering*. 2017 Dec 10; 13(4): 362-73. Doi: 10.22068/IJEEE.13.4.362
 20. Jabbari A, Shakeri M, Niaki SN. Pole shape optimization of permanent magnet synchronous motors using the reduced basis technique. *Iranian Journal of Electrical and Electronic Engineering*. 2010 Mar 10; 6(1): 48-55. Doi: 20.1001.1.17352827.2010.6.1.5.3
 21. Jabbari A, Shakeri M, Gholamian AS. Rotor pole shape optimization of permanent magnet brushless DC motors using the reduced basis technique. *Advances in electrical and computer engineering*. 2009 Jun 2; 9(2): 75-81. Doi:10.4316/AECE.2009.02012
 22. Jabbari A, Shakeri M, Nabavi NS. Torque ripple minimization in PM synchronous motors using tooth shape optimization. 2010; 27-31. URL: www.sid.ir/EN/VEWSSID/J_pdf/1000820100204.pdf
 23. Jabbari A, Shakeri M, Niaki AN. Iron pole shape optimization of IPM motors using an integrated method. *Advances in Electrical and Computer Engineering Journal*. 2010 Feb 27; 10(1). Doi:10.4316/AECE.2010.01012
 24. Kavanagh DF, Gyftakis KN, McCulloch MD. Early-onset degradation of thin-film magnet wire insulation for electromechanical energy converters. In 2019 IEEE 12th International Symposium on Diagnostics for Electrical Machines, Power Electronics and Drives (SDMPED) 2019 Aug 27; 37-43. Doi: 10.1109/DEMPED.2019.8864916
 25. Du Y, Xu C, Chen H, Xiao F, Zhu X, Zhang C, Xu L, Quan L. Low harmonics design for modular permanent magnet synchronous machine using partitioned winding. *IEEE Transactions on Industrial Electronics*. 2021 Sep 15; 69(9): 9268-78. Doi: 10.1109/TIE.2021.3111584
 26. Petrov I, Lindh P, Niemelä M, Scherman E, Wallmark O, Pyrhönen J. Investigation of a direct liquid cooling system in a permanent magnet synchronous machine. *IEEE Transactions on Energy Conversion*. 2019 Nov 8; 35(2): 808-17. Doi: 10.1109/TEC.2019.2952431
 27. Eastham JF, Profumo F, Tenconi A, Hill-Cottingham R, Coles P, Gianolio G. Novel axial flux machine for aircraft drive: design and modeling. *IEEE transactions on magnetics*. 2002 Sep; 38(5): 3003-5. Doi: 10.1109/TMAG.2002.803186
 28. El-Hasan TS, Luk PC, Bhinder FS, Ebaid MS. Modular design of high-speed permanent-magnet axial-flux generators. *IEEE Transactions on magnetics*. 2000 Sep; 36(5): 3558-61. Doi: 10.1109/20.908897

COPYRIGHTS

©2024 The author(s). This is an open access article distributed under the terms of the Creative Commons Attribution (CC BY 4.0), which permits unrestricted use, distribution, and reproduction in any medium, as long as the original authors and source are cited. No permission is required from the authors or the publishers.

**Persian Abstract****چکیده**

در این مقاله، یک نمونه ژنراتور مغناطیس دائم شار محور با توان ۳۰ کیلووات برای کاربری در یک توربین بادی درایو مستقیم طراحی و پارامترهای طراحی با هدف دستیابی به بازده بالا بهینه‌سازی شده است. به منظور کاهش گشتاور دندانه‌ای و ریپل گشتاور الکترومغناطیس، طرح ژنراتور هسته هوایی استفاده شده است و با هدف امکان افزایش ظرفیت توان ژنراتور، از ساختار مدولار استفاده شده است. مزیت طرح مدولار آن است که می‌توان هر ماژول را به عنوان یک واحد ژنراتور در نظر گرفت و بسته به شرایط سرعت باد، تعداد واحدهای متناسب با سرعت باد را در مدار قرار داد و همواره ژنراتور با بیشینه بازده کار کند. نخست با بهره‌گیری از معادلات حاکم، ابعاد و مشخصات عملکرد ژنراتور تعیین شده و سپس بر اساس طراحی الکترومغناطیس و مکانیکی، یک نمونه ژنراتور ساخته شده است. برای ارزیابی عملکرد خروجی ژنراتور، شبیه‌سازی ماشین در نرم افزار تحلیل اجزاء محدود ماکسول انجام شده و منحنی‌های مشخصه ولتاژ، جریان و تلفات اهمی آن استخراج شده است. به منظور ارزیابی دقت نتایج، نتایج حاصل از روش تحلیلی با نتایج آزمایشگاهی مقایسه شده است.